Computers and Concrete, *Vol. 19, No. 5 (2017) 443-449*
DOI: https://doi.org/10.12989/cac.2017.19.5.443

Experimental study on deformation of concrete for shotcrete use in high geothermal tunnel environments

Shengai Cui[1a], Pin Liu[2b], Xuewei Wang[*2], Yibin Cao[1c] and Yuezhong Ye[1d]

[1]*Department of Building Materials, School of Civil Engineerng, Southwest Jiaotong University, 610031, Chengdu, China*
[2]*Department of Bridge Engineering, School of Civil Engineering, Southwest Jiaotong University, 610031, Chengdu, China*

(Received April 1, 2016, Revised November 8, 2016, Accepted November 9, 2016)

Abstract. Taking high geothermal tunnels as background, the deformation of concrete for shotcrete use was studied by simulating hot-humid and hot-dry environments in a laboratory. The research is made up by two parts, one is the influence of two kinds of high geothermal environments on the deformation of shotcrete, and the other is the shrinkage inhibited effect of fiber materials (steel fibers, polypropylene fibers, and the mixture of both) on the concrete in hot-dry environments. The research results show that: (1) in hot and humid environments, wet expansion and thermal expansion happened on concrete, but the deformation is smooth throughout the whole curing age. (2) In hot and dry environments, the concrete suffers from shrinkage. The deformation obeys linear relationship with the natural logarithm of curing age in the first 28 days, and it becomes stable after the 28th day. (3) The shrinkage of concrete in a hot and dry environment can be inhibited by adding fiber materials especially steel fibers, and it also obeys linear relationship with the natural logarithm of curing age before it becomes stable. However, compared with no-fiber condition, it takes 14 days, half of 28 days, to make the shrinkage become stable, and the shrinkage ratio of concrete at 180-day age decreases by 63.2% as well. (4) According to submicroscopic and microscopic analysis, there is great bond strength at the interface between steel fiber and concrete. The fiber meshes are formed in concrete by disorderly distributed fibers, which not only can effectively restrain the shrinkage, but also prevent the micro and macro cracks from extending.

Keywords: high geothermal tunnel; hot-dry environment; shotcrete; deformation; fiber material

1. Introduction

With the development of tunnel construction toward longer, larger and deeper tunnels, thermal damage caused by high geothermal has become increasingly prominent (Wilhelm and Rybach 2003, Hochstein and Prebble 2006, Chen 2014, Zhao *et al*. 2014). High geotherm in tunnel construction is mainly in two forms. The first is hot and humid environments, where there exists fractures, or rock crashes that underground hot water could be easily gathered, which leads to hot springs. Cui *et al.* (2016) has explored the bond performance between shotcrete and rock in hot and humid tunnel environments by the experimental study. While the second is hot and dry environments, where there are better geological formations and the internal heat of geological layer spreads to the tunnel surface through the rocks. Cui *et al*. (2015) and Tang *et al*. (2015) has proved the severe influence of hot and dry environments on bond strength of shotcrete. The hardening process of shotcrete is accompanied by volume change, and the greatest deformation occurs when shotcrete shrinks in the air or other medium without sufficient humidity. It is obviously that, in a hot and dry environment, quick water lossing of shotcrete will cause great dry shrinkage, which will directly weaken the bonding strength between shotcrete and rock, and may even cause the failure of supporting function, even becoming the key factor to limit the application of shotcrete in high geothermal environments. Therefore, researching on shotcrete deformation performance in high geothermal environments has important engineering significance.

At present, to address the issue of high geothermal tunnels, much research has mainly focused on improving the tunnel environment by taking external or temporary measures such as ventilation cooling or artificial refrigeration cooling (Zhao and Yan 2001, Gu 2007, He 2009, Li and Dai 2011, Hou *et al*. 2013, Su 2014). However, few studies examined the material properties and its improvement measure in high geothermal environments. This study investigates the influence of high geothermal environments by simulating them in the laboratory. Meanwhile, considering the great shrinkage of shotcrete in hot and dry environments, it also explores the improvement effect of adding fiber materials, and analyzes its mechanism by submicroscopic and microscopic analysis.

∗Corresponding author, Ph.D. Student
E-mail: wxw5778@163.com
[a]Associate Professor
E-mail: shengai_cui@126.com
[b]Ph.D. Student
E-mail: 971907773@qq.com
[c]Postgraduate
E-mail: 674100095@qq.com
[d]Professor
E-mail: yeyazong@swjtu.edu.cn

ISSN: 1598-8198 (Print), 1598-818X (Online)

Table 1 Mix proportion for shotcrete C25

Cement (kg/m^3)	Sand (kg/m^3)	Gravel (kg/m^3)	Water (kg/m^3)	Accelerator (kg/m^3)	Water reducer (kg/m^3)
400	784	696	196	20	4.00

Table 2 Raw materials of shotcrete

Material	Cement	Sand	Gravel	Water-reducer	Accelerated agent
Type	P.O42.5R	Machine-made sand, medium sand with 2 % stone powder content	5-10 mm continuous grading	TK-SP polycarboxylic acid type	Alkali-free liquid BASF type

(a) Determination of slump (b) Casting fresh concrete

Fig. 1 Molding specimen

2. Experiment design

2.1 Design of basic mix proportion

The designed shotcrete strength is grade C25. The water-cement ratio (W/C) is determined as 0.49, sand ratio (β_s) as 55%, cement-aggregate ratio ($m_{c0}/(m_{s0}+m_{g0})$ as 1.0: 3.7, cement mass (m_{c0}) as 400 kg/m^3. According to the specifications (GB50086 2001), the basic mix proportion (i.e., without fiber material) is shown in Table 1. The raw materials for the shotcrete mix are shown in Table 2, and among them the initial setting time of accelerated agent is 4 min24s and the final setting time is 10 min23s. The slump of concrete is 90 mm by test.

Because shotcrete specimens are large-scale, high-cost and time-consuming to be prepared in specialized company, it is advisable to perform exploratory test on the specimens casted with molds (Leung *et al*. 2005). For this laboratory investigation, shotcrete was substituted with cast concrete with a composition equal to that of shotcrete used for spraying. The cast concrete specimens here were molded by vibrating technology with concrete vibrating table, shown in Fig. 1.

2.2 Simulating high geothermal environments

An accurate simulation of curing condition for molded specimens is a basic guarantee for studying shotcrete deformation in a high geothermal environment. During the experiments, constant temperature oven and constant temperature water tank are respectively used to simulate hot and dry environments (shown in Fig. 2(a)) and hot and humid environments (shown in Fig. 2(b)).After form removal, the specimens are rapidly moved into the water tank or oven at specified temperatures for curing until the defined curing age. Then the specimens are moved out and the lengths of them are rapidly measured within 15 s. After that, they are taken into the water tank or oven to be cured continuously.

(a) Hot-dry environment (b) Hot-humid environment

Fig. 2 Simulating high geothermal environment

Fig. 3 Measuring concrete deformation

2.3 Measuring deformations of concrete specimens

The experimental study of concrete deformation is carried out with contact method (Ministry of Housing and Urban-Rural Development of the People's Republic of China 2009) .The specimens are prisms with a dimension of 100 mm×100 mm×515 mm and each three of them come to a group. The stainless steel probes are embedded on both sides of the specimens, and the deformation is measured by horizontal contraction instrument.

Molded specimens should firstly be placed in the environment with temperature of (20±2)℃ and relative humidity of (60±5)%. Form removal is performed after final setting of concrete, and its initial length should be measured immediately at that moment. Then the specimens should be quickly moved into curing boxes. The subsequent length of the specimens will be measured at pecified intervals: 1 day, 3 days, 7 day, 14 days, 28 days, 45 days, 60 days, 90 days, 120 days, 150 days and 180 days. Measurement of concrete deformation is shown in Fig. 3.

The concrete shrinkage rate should be calculated according to the following formula

Table 3 Deformation of concrete in different curing conditions

Shrinkage Ratio Age (day)	Environment conditions				
	20℃-reference	50℃-oven	70℃-oven	50℃-water tank	70℃-water tank
0	0.00E+00	0.00E+00	0.00E+00	0.00E+00	0.00E+00
1	1.40E-04	-1.19E-04	-2.89E-04	-3.82E-04	-5.75E-04
3	2.06E-04	6.59E-05	-4.12E-05	-3.99E-04	-5.95E-04
7	3.00E-04	2.89E-04	2.10E-04	-3.70E-04	-5.69E-04
14	3.86E-04	3.92E-04	2.68E-04	-3.56E-04	-6.27E-04
21	4.83E-04	5.08E-04	3.76E-04	-3.59E-04	-5.92E-04
28	5.72E-04	5.99E-04	3.98E-04	-3.14E-04	-6.35E-04
45	5.80E-04	6.23E-04	4.04E-04	-3.68E-04	-6.57E-04
60	6.95E-04	5.94E-04	3.96E-04	-4.00E-04	-7.42E-04
90	6.64E-04	6.31E-04	4.06E-04	-3.28E-04	-7.36E-04
120	6.92E-04	6.13E-04	3.89E-04	-3.77E-04	-6.74E-04
150	7.37E-04	6.56E-04	4.44E-04	-2.85E-04	-5.74E-04
180	7.73E-04	6.95E-04	4.48E-04	-2.83E-04	-6.26E-04

$$\varepsilon_{st} = \frac{L_0 - L_t}{L_b} \quad (1)$$

Note:

ε_{st}-Concrete shrinkage ratio at t (day) age;

L_b-Measured gage length of specimen. It is equal to the value that concrete specimen length (excluding the protruding part of probes) subtracts the buried depth sum of the two probes (mm);

L_0-Initial length of concrete specimen (mm);

L_t-Length of specimen at t (day) age (mm);

The arithmetic average of shrinkage ratios of the 3 specimens are taken as the shrinkage ratio of this group of concrete specimens.

3. Influence of high geothermal environments on concrete deformation

There are many factors affecting the deformation of concrete, such as the amount of cementing materials, varieties of cement, water-cement ratio, elastic modulus of aggregate, etc. However, the influence of high geothermal environments can be emphatically analyzed in this experiment in the given conditions of raw material and mix proportion. The main non-loaded deformation forms of concrete including chemical shrinkage, dry shrinkage, wet expansion, and temperature deformation. The experiment results is actually the comprehensive performance of several forms above, therefore, the early deformation and the long-term deformation of concrete could be reflected in a certain extent.

The experimental environment conditions are set as follows: (1) 20℃ temperature and 60% relative humidity (denoted by 20℃-reference); (2) 50℃ constant temperature water tank (denoted by 50℃-water tank); (3) 50℃ constant temperature oven(denoted by 50℃-oven); (4) 70℃ constant temperature water tank (denoted by 70℃-water tank); (5) 70℃ constant temperature oven (denoted by 70℃-oven).

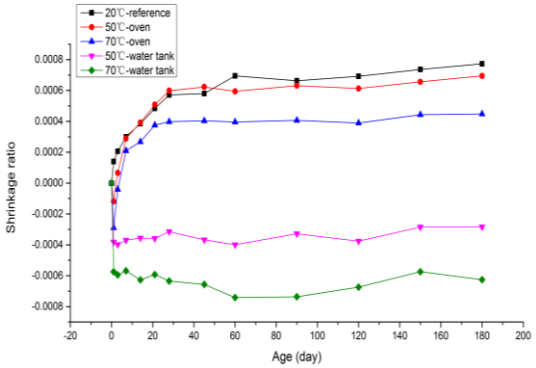

Fig. 4 Deformation curves of concrete in different curing conditions

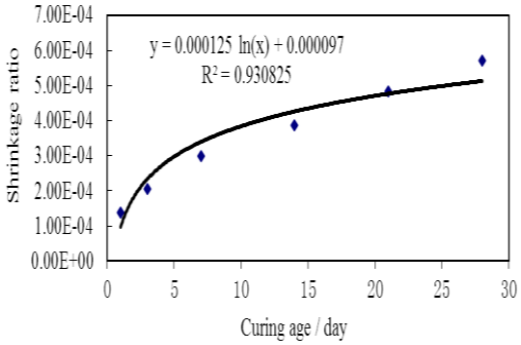

(a) 20℃-reference

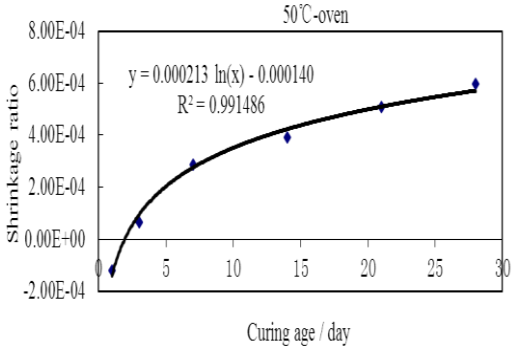

(b) 50℃-oven

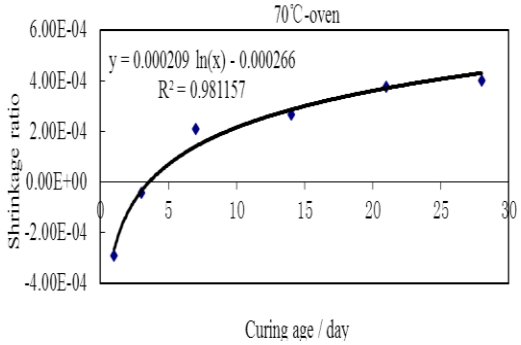

(c) 70℃-oven

Fig. 5 Fitted curves between shrinkage ratio and curing age before becoming stable (before 28 days)

According to Table 3 and Fig. 4, the deformation results

Table 4 Deformation results of concrete for added fiber materials conditions

Shrinkage Ratio Age (day)	Conditions			
	70℃-BP-oven	70℃-SF-oven	70℃-PF-oven	70℃-DF-oven
0	0.00E+00	0.00E+00	0.00E+00	0.00E+00
1	-2.89E-04	-2.57E-04	-2.55E-04	-2.48E-04
3	-4.12E-05	-9.14E-05	-2.82E-06	-9.34E-06
7	2.10E-04	1.07E-04	2.02E-04	1.56E-04
14	2.68E-04	1.87E-04	2.92E-04	2.85E-04
21	3.76E-04	1.84E-04	3.00E-04	2.80E-04
28	3.98E-04	1.84E-04	3.02E-04	2.98E-04
45	4.04E-04	1.66E-04	2.63E-04	2.74E-04
60	3.96E-04	1.60E-04	3.09E-04	3.23E-04
90	4.06E-04	1.53E-04	3.13E-04	3.10E-04
120	3.89E-04	1.58E-04	3.27E-04	3.21E-04
150	4.44E-04	1.62E-04	3.42E-04	3.31E-04
180	4.48E-04	1.65E-04	3.40E-04	3.28E-04

of concrete specimens in 5 different environment conditions can be analyzed horizontally. Compared with initial length (0 day), concrete shrinks in 20℃-reference and hot-dry conditions (namely 70℃-oven and 50℃-oven), while expanding in hot-humid conditions (namely 50℃-water tank and 70℃-water tank). Affected by temperature and humidity synthetically, the shrinkage ratio of 20℃-reference is a little lower than that of 50℃-oven since the 7th day to the 45th day, and it surpasses the 50℃-oven slightly after the 60th day. However, both of them are larger than the ratio of 70℃-oven, which may be due to the greater thermal expansion. For hot and humid environments, the expansion ratio of 70℃-water tank is higher than 50℃-water tank at each age, and it is about twice as high as 50℃-water tank since the 28th day.

Longitudinal analysis for each condition as follows: (1) the concrete of 50℃-water tank and 70℃-water tank are in expansion state during the whole curing period, and the overall trend are relatively stable. The expansion ratio in the 50℃-water tank is 2.83E-04 at 180-day age, while the 70℃-water tank is 6.26E-04 at the same age. (2) The concrete of 20℃-reference keeps shrinking throughout the entire testing time. But it has a greatly growing stage in the first 28 days, obeying linear relationship with the natural logarithm of curing age (shown in Fig. 5(a)). After 28 days, the deformation of concrete tends to be stable, and the shrinkage ratio reaches 7.73E-04 at 180-day age. (3) The concrete of 50℃-oven is in a slight expansion state at 1-day age, but it has tend to shrink since the 3rd day. Also the shrinkage ratio has the same regular with 20℃-reference, growing rapidly in the first 28 days, obeying linear relationship with the natural logarithm of curing age (shown in Fig. 5(b)), and becoming stable in the next days, the shrinkage ratio reaches 6.95E-04 at 180-day age. (4) The concrete of 70℃-oven has obvious expansion at the beginning, its expansion ratio reaches 2.89E-04 in the first day, and it still slightly expands at 3-day age. It is until the 7th day that the concrete comes to the shrinkage state. Also,

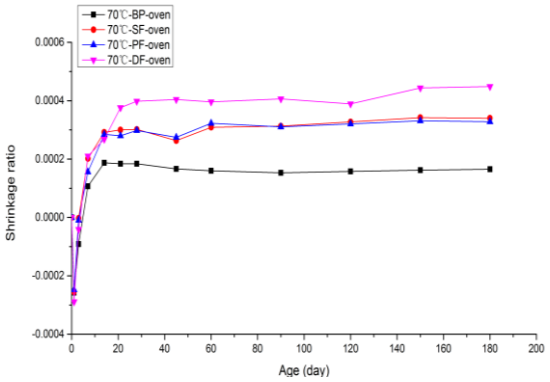

Fig. 6 Deformation curves of concrete in different curing conditions

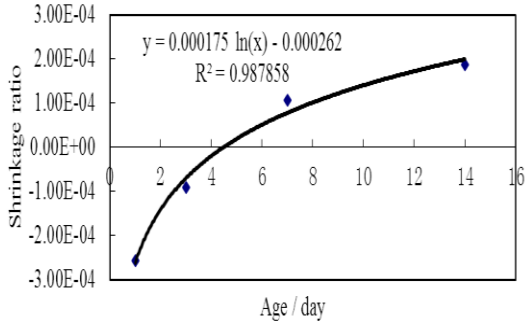

(a) 70℃-SF-oven

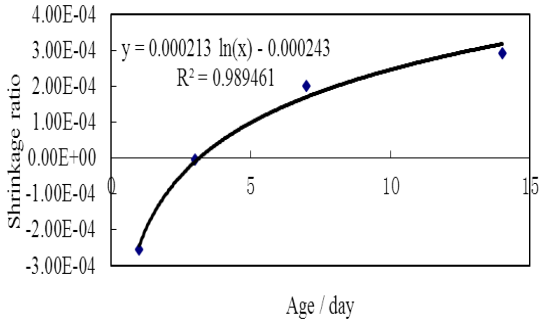

(b) 50℃-PF-oven

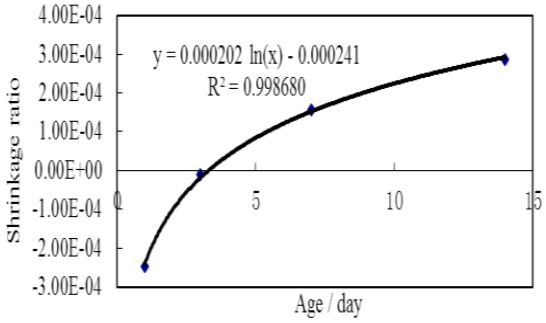

(c) 70℃-DF-oven

Fig. 7 Fitted curves between shrinkage ratio and curing age before becoming stable (before 14 days)

the shrinkage ratio of concrete obeys linear relationship with the natural logarithm of curing age (shown in Fig. 7(c)) and grows quickly before the age of 28. After that, the deformation ratio tends to be stable, reaching to 4.48E-04 on the 180th day. From above, there are similar deformation trends for concrete in these environment conditions (20℃-

Fig. 8 Submicroscopic structure of 70℃-BP-oven

Fig. 9 Submicroscopic structure of 70℃-SF-oven

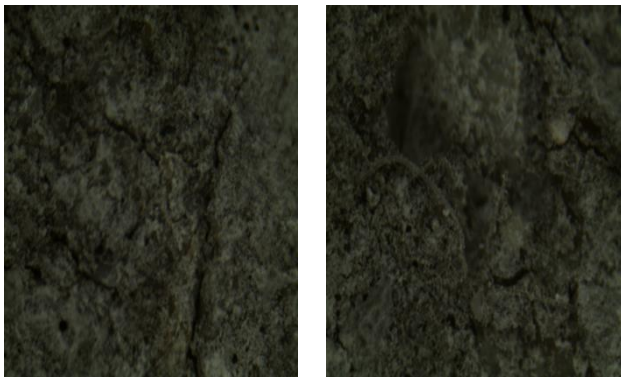

(a) (b)

Fig. 10 Submicroscopic structure of 70℃-PF-oven

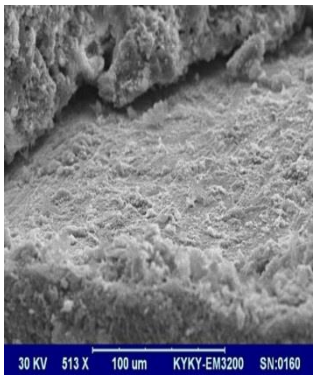

(a) Steel fiber embedded in concrete

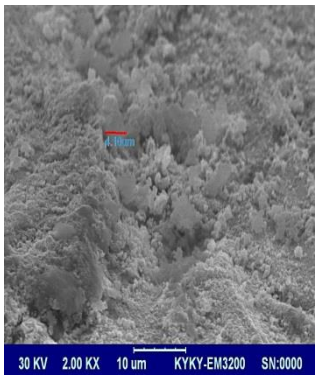

(b) Hydration products on the surface of the steel fiber

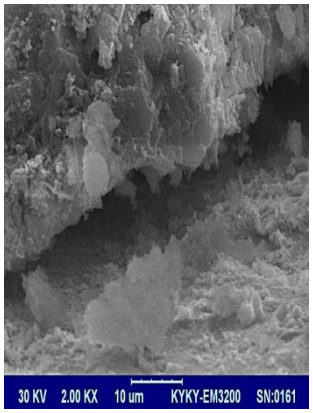

(c) Interface between steel fiber and concrete

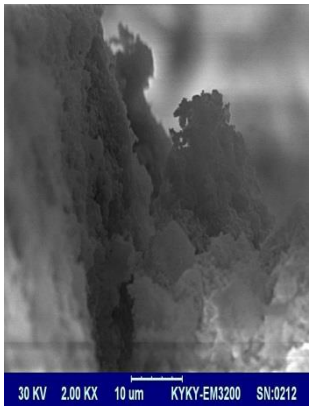

(d) Hydration products in the interface

Fig. 11 Micro-structures of 70℃-SF-oven

reference, 50℃-oven and 70℃-oven). It is clear that the concrete are all in shrinking stage from the whole perspective, their deformation tends to be stable after 28 days, and obeys linear relationships with the natural logarithm of curing age before the age of 28.

In conclusion, due to the micro-structure and meso-structure degradation of cement-based material caused by too fast temperature rising and water loss, physical and chemical shrinkage of concrete, and non-uniform temperature effects of interface between cement and aggregate, the influence mechanism of temperature on the shrinkage in hot-dry environments ratio is very complex. Because water losing is much more seriously in 70℃-oven than in 50℃-oven, so the 70℃-oven will be considered as the representative condition to explore the measures which could reduce the shrinkage.

4. Influences of fiber materials on deformation property of concrete under a hot and dry environment

Under hot and dry environments, the shrinkage is great, which is adverse to the bonding strength between shotcrete and rock. The influences of fiber materials (steel fibers, polypropylene fibers, mixture of both) on deformation performance of concrete in such environment are studied, which is aimed to put forward theoretical reference for improving the bonding strength of shotcrete. The following fibers were added into the raw materials listed in Table 2: steel fiber (cutting indentation type, 0.7×1×35 mm), and polypropylene fiber (PF) (length 20 mm, density 0.91 g/cm^3). With 70℃ hot and dry environment as background, Three different working conditions are conducted for the research under 70℃ hot-dry environment: 1% (volume ratio) of steel fiber mixed (70℃-SF-oven), 0.9 kg/m^3 of polypropylene fiber mixed (70℃-PF-oven), Double mix of 1% (volume ratio) of steel fibers and 0.9 kg/m^3 of polypropylene fiber (70℃-DF-oven). During the 180 days observation period, the deformation results of these working conditions are recorded in Table 4, and the corresponding curves are plotted in Fig. 6.

Compared with 70℃-BP-oven in Fig. 6, the shrinkages of concrete with fibers (i.e., 70℃-SF-oven, 70℃-PF-oven and 70℃-DF-oven) has all decreased to some extent, which indicates different fiber materials are all playing a certain role in inhibiting the shrinkage in hot-dry environment. No matter what kind of working conditions, the shrinkage ratio of concrete is obviously growing before 14 days, and it obeys linear relationship with the natural logarithm of curing age (shown in Fig. 7). After 14 days, the deformation of concrete tends to be stable. Among them, the shrinkage ratio of 70℃-SF-over is the smallest.

The experimental results above could be analyzed longitudinally with curing age: On the 1st day, all specimens are in expansion state with almost the same rate. On the 3rd

day, they are still in the state of expansion, however, the ratios of 70℃-PF-oven and 70℃-DF-oven conditions already became very low, which are respectively 2.82E-06 and 9.34E-06, while that of 70℃-SF-oven is in a higher magnitude, reaching to 9.14E-05. All the specimens have entered shrinkage states from the 7^{th} day. On the 14^{th} day, the shrinkage ratios of three conditions (70℃-SF-oven, 70℃-PF-oven, and 70℃-DF-oven) are respectively 1.87E-04, 2.92E-04 and 2.85E-04. After this curing age, the shrinkage ratio of concrete tends to be stable. When it reaches to the 180^{th} day, the shrinkage ratios of 70℃-PF-oven and 70℃-DF-oven are 3.40E-04 and 3.28E-04 respectively, nearly twice as much as that of 70℃-SF-oven which is 1.65E-04.

Above all, the shrinkage of the specimens with fibers all decreased, meanwhile, the curing age when shrinkage curves tend to be stable changes from 28 days to 14 days. All these show that the fiber materials play an important role in reducing shrinkage of concrete in hot and dry environment, especially with steel fibers. Though polypropylene fiber also has a good effect, it performs much badly than steel fiber. It is maybe because that the polypropylene fiber will degrade or even come to aging under hot and dry environment for its organic nature.

5. Submicroscopic analysis and microscopic analysis

To analyze the improvement effect of steel fiber at the mesoscopic aspect, the submicroscopic tests are carried out with light microscope. The submicroscopic morphologies of 70℃-BP-oven, 70℃-SF-oven and 70℃-PF-oven are showed and showed in Fig. 8, Fig. 9 and Fig. 10 respectively. Compared with Fig. 8 and Fig. 10, the morphology of concrete in Fig. 9 is more compacted and almost no clear cracks can be seen due to the inhibiting effect of steel fibers on cracks. While, there are a lot of cracks in concrete section in Fig. 10. Besides, when ontrasted with the initially mixed amount when molding specimens for this condition, the number of visible polypropylene fibers in concrete section reduces significantly and the toughness of fibers contrasted with the initially mixed amount when molding specimens for this condition, the number of visible polypropylene fibers in concrete section reduces significantly and the toughness of fibers decreases by on-site observation. This can explain the polypropylene fibers are less than steel fibers on the limiting shrinkage of concrete in 70℃ hot-dry environments.

The micro-structures of 70℃-SF-oven can be further observed by SEM. Fig. 11(a) shows the steel fiber embedding in concrete; Fig. 11(b) shows the hydration products on the surface of steel fiber; Fig. 11(c) shows the interface between steel fiber and concrete; Fig. 11(d) shows the hydration products on the interface between steel fibers and concrete. All these above indicate that there is great interfacial bonding force between steel fibers and concrete, and the development of cracks could be stopped in a certain extent by the interaction of interfacial bonding force, friction force mechanical force caused by steel fibers.

In conclusion, the reason why steel fibers can inhibit the shrinkage of concrete could be explained as follows: Firstly, uniformly distributed steel fiber meshes with small space are formed in concrete matrix. Therefore, when the shrinkage stress occurs in concrete matrix as a result of shrinkage deformation, the fiber meshes prevent it from shrinking. Secondly, the incurrence of primary cracks and the extension of secondary cracks can be both reduced due to the crack resistance effect of steel fibers, so the shrinkage caused by the capillary pressure has also been lowered to some extent. Thirdly, in hot and dry environments, internal heat could be evenly distributed because of the high thermal conductivity of steel fibers.

6. Conclusions

Based on the analysis and experimental study presented in this paper, the following conclusions may be drawn:

• In hot and humid environments, the concrete suffers from wet expansion and thermal expansion, and the overall trend of the deformation is stable with the increase of curing age. However, in hot and dry environments, the concrete shrinks, and it obeys linear relationship with the natural logarithm of curing age in the first 28 days, then becomes stable in the next ages.

• The shrinkage of concrete in hot and dry environments can be inhibited by adding fiber materials especially steel fibers. Compared with basic mix proportion (i.e., without fiber material, denoted by BP), the deformation also obeys linear relationship with the natural logarithm of curing age before becoming stable, but the curing age when the shrinkage tends to be stable changes from 28 days to 14 days. Moreover, the shrinkage ratio of concrete at 180-day age decreased by 63.2%. For the condition with polypropylene fibers, it only decreased by 13.4% at the same age.

• Submicroscopic and microscopic results show steel fibers can restrict the shrinkage effectively with the help of great interfacial bonding forces between steel fibers and concrete. Besides, friction forces and mechanical interaction forces, which work together with the bonding forces, can also stop or block the development of cracks.

• Although there are different shrinkage ratios for shotcrete considering its different composition and strength grade, the general trend remains similar as is shown in this paper. However, there is only 20℃, 50℃ and 70℃ data in this paper, more temperatures' data will be studied in the future work.

Acknowledgments

We would like to acknowledge the National Natural Science Foundation of China (grant no. 51678492).

References

Chen, G.Q., Li, T.B., Zhang, G.F., Yin, H.Y. and Zhang, H. (2014), "Temperature effect of rock burst for hard rock in deep-

buried tunnel", *Nat. Haz.*, **72**(2), 915-926.
Cui, S.A., Li, J.W., Ye, Y.Z. and Yang, H.Y. (2013), "Bond strength of shotcrete with rock in dry and hot environment of high ground temperature tunnel", *J. Build. Mater.*, **16**(4), 663-666.
Cui, S.A., Zhu, B., Li, F.H. and Ye, Y.Z. (2016), "Experimental study on bond performance between shotcrete and rock in hot and humid tunnel environment", *KSCE J. Civil Eng.*, **20**(4), 1385-1391.
GB50086 (2001), *Specifications for Bolt-Shotcrete Support*, Beijing, China.
Gu, B.S. (2007), "Counter measures against high temperature in a tunnel and the corresponding ventilation design-feasibility study for the super-long gaoligongshan tunnel", *Mod. Tunnel. Technol.*, **44**(2), 66-71.
He, M.C. (2009), "Application of HEMS cooling technology in deep mine heat hazard control", *Min. Sci. Techonol.*, **19**(3), 269-275.
Hochstein, M.P. and Prebble, W.M. (2006), "Major engineering constructions on top of a high-temperature geothermal system: Problems encountered at Tokaanu", *Geotherm.*, **35**(4), 428-447.
Hou, D.P., Liu, N.F., Yu, C.M. and Li, N. (2013), "Discussion on design and construction measures for a rock tunnel in high-temperature conditions", *Chin. J. Rock Mech. Eng.*, **32**(2), 3396-3402.
Leung, C.K., Lai, R. and Lee, A.Y.F. (2005), "Properties of wet-mixed fiber reinforced shotcrete and fiber reinforced concrete with similar composition", *Cement Concrete Res.*, **35**(4), 788-795.
Li, X.Q. and Dai, L.X. (2011), "Cooling technology for construction of high earth temperature section of a diversion tunnel", *Wat. Res. Hydropow. Eng.*, **42**(2), 36-41.
Ministry of Housing and Urban-Rural Development of the People's Republic of China GB/T 50082 (2009), *Standard for Test Methods of Long-Term Performance and Durability of Ordinary Concrete*, China Architecture & Building Press, Beijing, China.
Su, H. (2014), "Hydropower tunnel in high geothermal condition: Influences of high ground temperature and countermeasures", *Tunn. Constr.*, **34**(4), 351-355.
Tang, Y., Su, H., Zhang, H., Ma, Q.J. and Jiang, T. (2015), "Cohesive strength and micro failure mechanism of high geothermal diversion tunnel shotcrete surrounding rock", *Wat. Res. Pow.*, **33**(4), 127-129.
Wilhelm, J. and Rybach, L. (2003), "The geothermal potential of Swiss alpine tunnels", *Geotherm.*, **32**(4), 557-568.
Yang, X.L. (2013), "Research on geothermal anomaly characteristics and control measures for Jiwoxiga tunnel on lasa-shigatse railway", *Rail. Stand. Des.*, **58**(7), 107-111.
Zhao, G.B., Li, G.Y.S., Qu, Z.Y. and Hu, X.B. (2014), "Particular engineering geological problems of diversion tunnel of qirehataer water power station", *Res. Environ. Eng.*, **28**(4), 411-413.
Zhao, T.X. and Yan, M.F. (2001), "Temperature lowering technique for hot water with high pressure in Heibaishui ladder-shaped power station tunnel", *Mod. Tunnel. Technol.*, **38**(3), 48-51.